

Shedding New Light on $\mathcal{R}(D_{(s)}^{(*)})$ and $|V_{cb}|$ from Semileptonic $\bar{B}_{(s)} \rightarrow D_{(s)}^{(*)} \ell \bar{\nu}_\ell$ Decays

Bo-Yan Cui,^{*} Yong-Kang Huang,[†] Yu-Ming Wang,[‡] and Xue-Chen Zhao[§]

School of Physics, Nankai University, Weijin Road 94, Tianjin 300071, P.R. China

(Dated: August 23, 2023)

We compute for the first time the next-to-leading-order QCD corrections to the $\bar{B}_{(s)} \rightarrow D_{(s)}^{(*)}$ form factors at large hadronic recoil. Both the charm-quark-mass and the strange-quark-mass dependent pieces can generate the leading-power contributions to these form factors. Including further various power-suppressed contributions, we perform the combined fits of the considered form factors to both our large-recoil theory predictions and the lattice QCD results, thus improving upon the previous determinations of the lepton-flavour-universality ratios $\mathcal{R}(D^{(*)})$ significantly.

INTRODUCTION

The flagship semileptonic $\bar{B}_{(s)} \rightarrow D_{(s)}^{(*)} \ell \bar{\nu}_\ell$ decay processes are of extraordinary phenomenological importance for the precise determination of the Cabibbo-Kobayashi-Maskawa (CKM) matrix element $|V_{cb}|$ and for probing the non-standard flavour-changing dynamics above the electroweak scale [1–6]. The persisting discrepancy between the exclusive and inclusive extractions of $|V_{cb}|$ at the level of $2\sigma \sim 3\sigma$ has triggered enormous efforts on uncovering the ultimate mystery of this intriguing puzzle in the Standard Model (SM) and beyond (see for instance [7–11]). Moreover, the state-of-the-art theory predictions for the two lepton-flavour-universality (LFU) ratios $\mathcal{R}(D^{(*)})$ [12] appear to be in tension with the HFLAV-averaged experimental measurements [13] (at the 3σ level when combined together) as well, thus stimulating intensive investigations on a wide range of other interesting LFU observables [14–22]. Apparently, disentangling the potential new physics (NP) signals from the unaccounted theoretical uncertainties in the SM computations in a robust manner will be indispensable for the unambiguous interpretation of these emerged flavour anomalies. It remains important to remark that the updated LHCb measurements for the electron-muon universality ratios $\mathcal{R}(K^{(*)})$ in the flavour-changing neutral current loop processes $B \rightarrow K^{(*)} e^+ e^-$ and $B \rightarrow K^{(*)} \mu^+ \mu^-$ [23, 24] do not necessarily lead to conclude the tauon-muon universality in the neutral current $b \rightarrow s l \bar{l}$ transitions [25, 26], let alone in the flavour-changing charged current tree decays $\bar{B}_{(s)} \rightarrow D_{(s)}^{(*)} \ell \bar{\nu}_\ell$ [27]. Actually, introducing new CP-violating couplings in the weak effective Hamiltonian for $b \rightarrow s l \bar{l}$ can bring about the significant space to violate the electron-muon universality, while accommodating the new LHCb result for the $\mathcal{R}(K)$ ratio simultaneously [28].

The model-independent descriptions of the heavy-to-heavy bottom-meson decay form factors in the low recoil regime can be naturally formulated by adopting the heavy quark effective theory (HQET) based upon an expansion in powers of $\Lambda_{\text{QCD}}/m_{b,c}$, yielding a tower of the

non-perturbative Isgur-Wise (IW) functions. In order to better constrain the desirable shape of these form factors, an attractive prescription to derive the unitarity constraints for the form-factor expansion coefficients has been developed from the fundamental field-theoretical principles [29–34]. Additionally, we have witnessed the substantial progress on the encouraging lattice QCD calculations of the $\bar{B} \rightarrow D^{(*)} \ell \bar{\nu}_\ell$ form factors [35–37] and the $\bar{B}_s \rightarrow D_s^{(*)} \ell \bar{\nu}_\ell$ form factors [38–40] at non-zero recoil. By contrast, the continuum QCD determinations of such fundamental heavy-to-heavy form factors at large recoil are mainly achieved by evaluating only the leading-order QCD contributions at the twist-four accuracy [41, 42], apart from the currently available higher-order QCD computations of the $\bar{B} \rightarrow D$ form factors [43, 44].

In view of the noticeable significance of implementing the large-recoil theory predictions in the numerical fit of the exclusive bottom-meson decay form factors [45–54], accomplishing the next-to-leading-order (NLO) computations to the semileptonic $\bar{B}_{(s)} \rightarrow D_{(s)}^* \ell \bar{\nu}_\ell$ form factors will therefore be in high demand for pinning down the obtained uncertainties of their shape parameters from the combined z -series fitting procedure. To achieve this goal, we will first establish the NLO factorization formulae for the appropriate bottom-meson-to-vacuum correlation functions at leading power (LP) in the soft-collinear effective theory (SCET) framework and then construct the large logarithmic resummation improved light-cone sum rules (LCSR) for the considered form factors. In particular, we will report on a novel observation of the LP $\mathcal{O}(\alpha_s)$ contribution to the longitudinal form factors due to the unsuppressed charm-quark mass dependent pieces in the SCET Lagrangian, when applying the preferable power-counting scheme $m_c \sim \mathcal{O}(\sqrt{\Lambda_{\text{QCD}} m_b})$ [55, 56]. Phenomenological implications of the simultaneous Boyd-Grinstein-Lebed (BGL) expansion fitting [29–31] to both the SCET sum rules predictions and the lattice simulation data points will be further explored with the focus on the updated extractions of the LFU quantities $\mathcal{R}(D_{(s)}^{(*)})$ and the CKM matrix element $|V_{cb}|$.

GENERAL ANALYSIS

We adopt the customary definitions of the bottom-meson decay form factors $\{V, A_0, A_1, A_2\}$ as displayed in [57]. Implementing the matching program QCD \rightarrow SCET_I for these form factors enables us to derive the factorization formulae in terms of the SCET form factors

$$\begin{aligned} \mathcal{V}(n \cdot p) &= C_V^{(A0)}(n \cdot p) \xi_{\perp}(n \cdot p) + C_V^{(A1, m_c)}(n \cdot p) \xi_{\perp, m_c}(n \cdot p) + \int_0^1 d\tau C_V^{(B1)}(\tau, n \cdot p) \Xi_{\perp}(\tau, n \cdot p) + \mathcal{V}^{\text{NLP}}(n \cdot p), \\ \mathcal{A}_0(n \cdot p) &= C_{f_0}^{(A0)}(n \cdot p) \xi_{\parallel}(n \cdot p) + C_{f_0}^{(A1, m_c)}(n \cdot p) \xi_{\parallel, m_c}(n \cdot p) + \int_0^1 d\tau C_{f_0}^{(B1)}(\tau, n \cdot p) \Xi_{\parallel}(\tau, n \cdot p) + \mathcal{A}_0^{\text{NLP}}(n \cdot p), \\ \mathcal{A}_1(n \cdot p) &= C_V^{(A0)}(n \cdot p) \xi_{\perp}(n \cdot p) + C_{A_1}^{(A1, m_c)}(n \cdot p) \xi_{\perp, m_c}(n \cdot p) + \int_0^1 d\tau C_V^{(B1)}(\tau, n \cdot p) \Xi_{\perp}(\tau, n \cdot p) + \mathcal{A}_1^{\text{NLP}}(n \cdot p), \\ \mathcal{A}_{12}(n \cdot p) &= C_{f_+}^{(A0)}(n \cdot p) \xi_{\parallel}(n \cdot p) + C_{f_+}^{(A1, m_c)}(n \cdot p) \xi_{\parallel, m_c}(n \cdot p) + \int_0^1 d\tau C_{f_+}^{(B1)}(\tau, n \cdot p) \Xi_{\parallel}(\tau, n \cdot p) + \mathcal{A}_{12}^{\text{NLP}}(n \cdot p). \end{aligned} \quad (1)$$

The newly introduced form factors \mathcal{V} , \mathcal{A}_0 , \mathcal{A}_1 and \mathcal{A}_{12} can be expressed in terms of the linear combinations of the conventional form factors as displayed in (1) of the Supplemental Material. The explicit definitions of $\xi_{\parallel, \perp}$ and $\Xi_{\parallel, \perp}$ take the same form as the ones for the exclusive heavy-to-light transitions [58], while the remaining two effective form factors ξ_{\parallel, m_c} and ξ_{\perp, m_c} can be defined by

$$\begin{aligned} \langle D_q^*(p, \epsilon^*) | (\bar{\xi} W_c) \frac{\not{m}_c}{2 - in \cdot \not{D}_c} \gamma_5 h_v | \bar{B}_v \rangle \\ = -n \cdot p (\epsilon^* \cdot v) \xi_{\parallel, m_c}(n \cdot p), \end{aligned} \quad (2)$$

$$\begin{aligned} \langle D_q^*(p, \epsilon^*) | (\bar{\xi} W_c) \frac{\not{m}_c}{2 - in \cdot \not{D}_c} \gamma_5 \gamma_{\mu \perp} h_v | \bar{B}_v \rangle \\ = -n \cdot p (\epsilon_\mu^* - \epsilon^* \cdot v \bar{n}_\mu) \xi_{\perp, m_c}(n \cdot p). \end{aligned} \quad (3)$$

The analytic expressions for the short-distance coefficients $C_i^{(A0)}$ and $C_i^{(B1)}$ (determined from [59, 60]) as well as $C_i^{(A1, m_c)}$ are collected in (2) of the Supplemental Material. We will therefore dedicate the next section to the transparent computations of the effective form factors at $\mathcal{O}(\alpha_s)$, including further the tree-level determinations of the next-to-leading power (NLP) corrections.

NLO CORRECTIONS TO THE FORM FACTORS

In analogy to the strategy for computing the heavy-to-light bottom-meson decay matrix elements [61, 62] (see also [63, 64]), we can derive the LCSR for $\xi_{\parallel}(n \cdot p)$ by exploring the particular SCET_I correlation function

$$\begin{aligned} \Pi_{\nu, \parallel}^{(A0)} &= \int d^4x e^{ip \cdot x} \langle 0 | T \{ j_{\xi q, \parallel \nu}^{(2)}(x), O_{\parallel}^{(A0)}(0) \} | \bar{B}_v \rangle \\ &+ \int d^4x e^{ip \cdot x} \int d^4y \\ &\langle 0 | T \{ j_{\xi \xi, \parallel \nu}^{(0)}(x), i\mathcal{L}_{\xi q}^{(2)}(y), O_{\parallel}^{(A0)}(0) \} | \bar{B}_v \rangle \end{aligned}$$

$$\begin{aligned} &+ \int d^4x e^{ip \cdot x} \int d^4y \int d^4z \\ &\langle 0 | T \{ j_{\xi \xi, \parallel \nu}^{(0)}(x), i\mathcal{L}_{\xi q}^{(1)}(y), i\mathcal{L}_{\xi m_c}^{(0)}(z), O_{\parallel}^{(A0)}(0) \} | \bar{B}_v \rangle \\ &+ \int d^4x e^{ip \cdot x} \int d^4y \\ &\langle 0 | T \{ j_{\xi \xi, \parallel \nu}^{(0)}(x), i\mathcal{L}_{\xi q, m_q}^{(2)}(y), O_{\parallel}^{(A0)}(0) \} | \bar{B}_v \rangle, \end{aligned} \quad (4)$$

where the manifest representations of $j_{\xi \xi, \parallel \nu}^{(0)}$, $j_{\xi q, \parallel \nu}^{(2)}$, $\mathcal{L}_{\xi q}^{(1)}$ and $\mathcal{L}_{\xi q}^{(2)}$ have been presented in [57, 65]. The remaining effective Lagrangian densities and the SCET_I weak current are presented in (3) of the Supplemental Material. Since the charm-quark mass dependent term $\mathcal{L}_{\xi m_c}^{(0)}$ describes the unsuppressed interaction between the collinear fields [66], the third term in the correlation function (4) will result in the power-enhanced contribution to the correlation function (4). Moreover, the spectator-quark mass contributions from the second and the fourth terms on the right-hand side of (4) can further give rise to the LP effects (see also [46, 66, 67]).

Matching the determined spectral representation of $\Pi_{\nu, \parallel}^{(A0)}$ with the corresponding hadronic dispersion relation leads to the desired NLO sum rules

$$\begin{aligned} \xi_{\parallel} &= 2 \frac{\mathcal{F}_{B_q}(\mu)}{f_{D_q^*, \parallel}} \frac{m_{B_q} m_{D_q^*}}{(n \cdot p)^2} \int_0^{\omega_s} d\omega' \exp \left[\frac{m_{D_q^*}^2 - n \cdot p \omega'}{n \cdot p \omega_M} \right] \\ &\left[\phi_{B, \text{eff}}^-(\omega') - \frac{m_c}{\omega'} \phi_{B, \text{eff}}^{+, m_c}(\omega') + \frac{m_q}{\omega'} \phi_{B, \text{eff}}^{+, m_q}(\omega') \right] \\ &\equiv \hat{\xi}_{\parallel} + \hat{\xi}_{\parallel}^{m_c} + \hat{\xi}_{\parallel}^{m_q}, \end{aligned} \quad (5)$$

where the two decay constants \mathcal{F}_{B_q} and $f_{D_q^*, \parallel}$ are defined with the conventions of [57]. The lengthy expressions for $\phi_{B, \text{eff}}^-$, $\phi_{B, \text{eff}}^{+, m_c}$ and $\phi_{B, \text{eff}}^{+, m_q}$ are summarized in the Supplemental Material. Remarkably, the SCET_I diagram (b) in Figure 1 of the Supplemental Material does not lead to

the power-enhanced contribution (but does generate the LP contribution) to the sum rules of ξ_{\parallel} after implementing *the continuum subtraction*. Applying the established computational strategy further allows for the construction of the SCET sum rules for the effective form factors ξ_{\parallel, m_c} and Ξ_{\parallel} (shown in (8) and (12) of the Supplemental Material) by investigating the appropriate correlation functions. Along the same vein, we can readily derive the NLO sum rules for the transverse form factors ξ_{\perp} , ξ_{\perp, m_c} and Ξ_{\perp} as collected in the Supplemental Material.

We then proceed to construct the subleading-power sum rules for the $\bar{B}_q \rightarrow D_q^*$ form factors from four distinct sources: I) the off-light-cone corrections from the two-body nonlocal HQET matrix elements, II) the yet higher-twist corrections from the three-particle B_q -meson distribution amplitudes [68, 69], III) the subleading-power corrections from the effective matrix element of $(\bar{\xi}W_c)\Gamma[iD_T/(2m_b)]h_v$ [65], IV) the higher-order terms from expanding the hard-collinear charm-quark propagator. The tree-level LCSR for the power-suppressed terms \mathcal{V}^{NLP} , $\mathcal{A}_0^{\text{NLP}}$, $\mathcal{A}_1^{\text{NLP}}$ and $\mathcal{A}_{12}^{\text{NLP}}$ will be presented explicitly in a forthcoming longer write-up.

NUMERICAL ANALYSIS

We are now in a position to explore phenomenological implications of the newly determined SCET sum rules with the three-parameter ansatz for the bottom-meson distribution amplitudes [70] (see also [71–77]), which fulfills simultaneously the non-trivial equations-of-motion constraints [70], the sum rule determinations of the two inverse moments $\lambda_{B_{d,s}}$ [78, 79] and the HQET parameters $\lambda_{E,H}^2$ [80–82], and the asymptotic behaviours at small quark and gluon momenta [69]. It is perhaps worth mentioning an attractive method for the first-principles determination of the B -meson light-cone distribution amplitude based upon the large momentum effective theory and the lattice simulation technique [83]. The leptonic decay constants of the pseudoscalar bottom mesons have been extracted from the lattice calculations precisely [84]. We further employ the QCD sum rule computations [85] for both the longitudinal and transverse D_q^* decay constants. The allowed intervals of the intrinsic LCSR parameters $M^2 = n \cdot p \omega_M$ and $s_0 = n \cdot p \omega_s$ are consistent with the previous determinations [86–89]. The choices for the additional parameters in our numerical studies are identical to the ones summarized in [46].

Inspecting the numerical features for the distinct classes of higher-order contributions indicates that the newly determined NLL QCD corrections can reduce the corresponding tree-level LP predictions by an amount of $\mathcal{O}(20\%)$. As displayed in Figure 1, the particular charm-quark mass dependent contribution $\hat{\xi}_{\parallel}^{m_c}$ in (5) appears to bring about the $\mathcal{O}(5\%)$ enhancement of the LP prediction of the form factor \mathcal{A}_0 with $q^2 \in [-3.0, 2.0] \text{ GeV}^2$. We

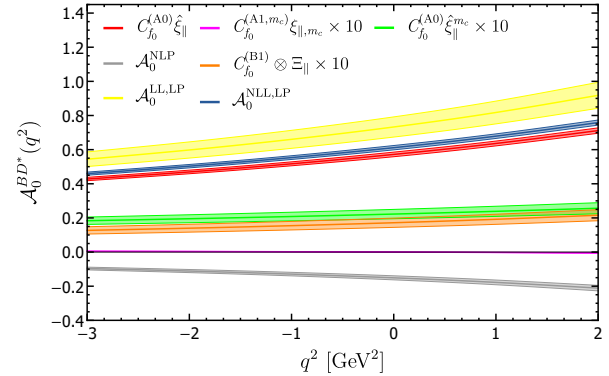


FIG. 1. Breakdown of the distinct dynamical mechanisms contributing to the form factor \mathcal{A}_0 for $\bar{B} \rightarrow D^* \ell \bar{\nu}_\ell$ in the kinematic range $q^2 \in [-3.0, 2.0] \text{ GeV}^2$ with the uncertainties from varying the hard and hard-collinear matching scales.

further note that the effective form factor ξ_{\parallel, m_c} defined in (2) can only result in the negligible impact on the numerical prediction for \mathcal{A}_0 in the large recoil region due to the kinematical suppression of the multiplication hard coefficient. It remains important to remark that the yielding uncertainties of our NLL \oplus NLP LCSR predictions arise, on the one hand, from the SCET computations of the bottom-meson-to-vacuum correlation functions and, on the other hand, from the extraction of the ground-state charmed meson contribution with the parton-hadron duality ansatz and the Borel transformation. In order to determine the mean values and theoretical uncertainties of the $\bar{B}_q \rightarrow D_q^*$ form factors, we employ the statistical procedure discussed in [90, 91] by simultaneously scanning the complete set of input parameters (displayed in Table I of the Supplemental Material) in the adopted intervals with the prior distribution. It is worthwhile mentioning further that the systematic uncertainty due to the parton-hadron duality ansatz has been addressed in a wide range of QCD computations (e.g., [92–101]), leading to the encouraging observation on the smallness of duality violations in the inclusive hadron production in $e^+ e^-$ annihilations [100], in the hadronic decays of the τ -lepton [101], and in the semileptonic bottom-meson decays [98]. In an attempt to obtain more conservative predictions of our SCET sum rules, we nevertheless increase the default intervals of the sum-rule parameters M^2 and s_0 by a factor of two in the ultimate error estimates. As elaborated further in the Supplemental Material, one of the principal benefits from our LCSR analysis consists in the yielding strong correlations between the LCSR data points at distinct q^2 -values, which are expected to be particularly insensitive to the duality approximation.

In order to extrapolate the LCSR predictions for the $\bar{B}_q \rightarrow D_q^*$ form factors towards the large momentum

Parameters	$\bar{B} \rightarrow D^{(*)}$ Form Factors			$\bar{B}_s \rightarrow D_s^{(*)}$ Form Factors		
	Lattice	Lattice \oplus LCSR	Lattice \oplus LCSR \oplus Exp.	Lattice	Lattice \oplus LCSR	Lattice \oplus LCSR \oplus Exp.
b_0^{f+}	0.0137 ± 0.0001	0.0137 ± 0.0001	0.0138 ± 0.0001	0.0041 ± 0.0001	0.0041 ± 0.0001	0.0042 ± 0.0001
b_1^{f+}	-0.0414 ± 0.0034	-0.0417 ± 0.0033	-0.0398 ± 0.0032	-0.0029 ± 0.0019	-0.0030 ± 0.0019	-0.0034 ± 0.0015
b_2^{f+}	0.1178 ± 0.2007	0.0415 ± 0.1124	0.1123 ± 0.0713	-0.0584 ± 0.0096	-0.0588 ± 0.0093	-0.0608 ± 0.0078
b_1^{f0}	-0.2064 ± 0.0155	-0.2072 ± 0.0147	-0.2004 ± 0.0144	-0.0610 ± 0.0112	-0.0617 ± 0.0111	-0.0571 ± 0.0108
b_2^{f0}	0.5572 ± 0.9626	0.1880 ± 0.5330	0.5581 ± 0.3297	-0.0264 ± 0.0768	-0.0233 ± 0.0767	-0.0359 ± 0.0756
b_0^g	0.0259 ± 0.0009	0.0256 ± 0.0009	0.0251 ± 0.0008	0.0080 ± 0.0009	0.0072 ± 0.0007	0.0071 ± 0.0007
b_1^g	-0.1093 ± 0.0786	-0.1005 ± 0.0456	-0.1104 ± 0.0396	0.0212 ± 0.0218	-0.0017 ± 0.0106	-0.0005 ± 0.0105
b_2^g	-0.4505 ± 4.3691	0.2587 ± 0.6564	0.2050 ± 0.6107	-0.0089 ± 0.1334	-0.1067 ± 0.0848	-0.0964 ± 0.0841
b_0^f	0.0108 ± 0.0002	0.0109 ± 0.0002	0.0106 ± 0.0002	0.0035 ± 0.0001	0.0036 ± 0.0001	0.0036 ± 0.0001
b_1^f	-0.0012 ± 0.0168	0.0081 ± 0.0101	0.0112 ± 0.0082	0.0041 ± 0.0036	0.0060 ± 0.0034	0.0059 ± 0.0032
b_2^f	-0.0379 ± 1.1507	0.0693 ± 0.2140	-0.0713 ± 0.1583	-0.0055 ± 0.0531	0.0287 ± 0.0447	0.0419 ± 0.0437
b_1^{F1}	-0.0046 ± 0.0031	-0.0024 ± 0.0020	0.0015 ± 0.0014	0.0013 ± 0.0009	0.0013 ± 0.0008	0.0019 ± 0.0007
b_2^{F1}	-0.0460 ± 0.1944	-0.0155 ± 0.0388	-0.0089 ± 0.0251	-0.0188 ± 0.0156	-0.0221 ± 0.0126	-0.0177 ± 0.0122
b_1^{F2}	-0.2949 ± 0.0742	-0.2097 ± 0.0581	-0.1364 ± 0.0490	-0.0078 ± 0.0190	-0.0093 ± 0.0145	0.0001 ± 0.0136
b_2^{F2}	0.5476 ± 4.0297	0.5667 ± 0.8789	0.5660 ± 0.7406	-0.2242 ± 0.1756	-0.1906 ± 0.1521	-0.1480 ± 0.1495
χ^2/dof	7.71/8	30.76/76	118.31/140	7.71/8	30.76/76	118.31/140
$R(D_q)$	0.3004 ± 0.0143	0.3066 ± 0.0081	0.2986 ± 0.0042	0.2993 ± 0.0046	0.2996 ± 0.0045	0.2971 ± 0.0042
$R(D_q^*)$	0.2718 ± 0.0300	0.2585 ± 0.0054	0.2500 ± 0.0016	0.2488 ± 0.0058	0.2506 ± 0.0040	0.2461 ± 0.0024

TABLE I. Theory predictions for the z -series expansion coefficients in the semileptonic $\bar{B}_{(s)} \rightarrow D_{(s)}^{(*)} \ell \bar{\nu}_\ell$ form factors determined by carrying out the BGL fitting against the “only lattice QCD” data points [35–37, 39, 40] (shown in the second and the fifth columns), by performing the simultaneous fitting to both the lattice QCD results [35–37, 39, 40] and the updated LCSR computations (shown in the third and the sixth columns), and by further implementing the available experimental data points [1, 3–5] in the combined BGL fit procedure (shown in the fourth and the last columns).

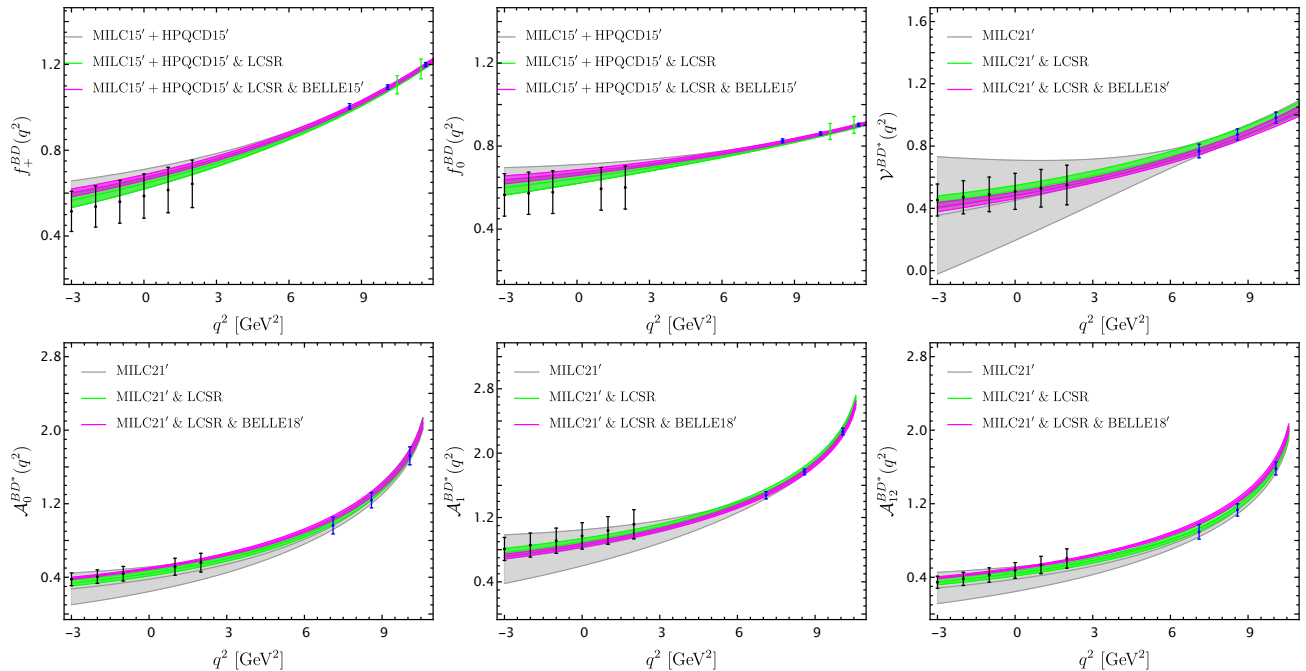


FIG. 2. Theory predictions for the momentum transfer dependence of the complete set of the exclusive $\bar{B} \rightarrow D^{(*)}$ form factors in the entire kinematic region from I) the BGL z -series fit against the “only lattice QCD” data points [35–37, 39, 40], II) the simultaneous fit to both the lattice QCD results [35–37, 39, 40] and our LCSR predictions, III) the combined numerical fit including further the available experimental data points [1, 3–5].

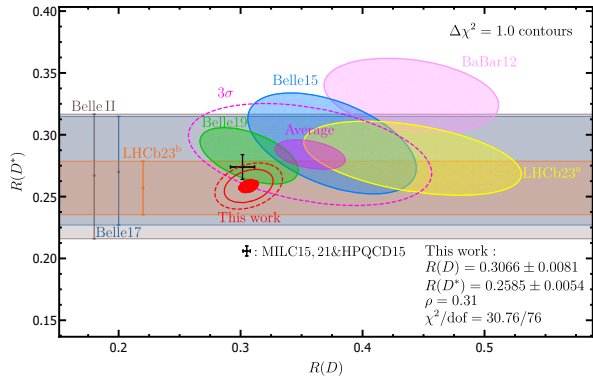


FIG. 3. The correlated theory predictions for $\mathcal{R}(D)$ and $\mathcal{R}(D^*)$ from the combined BGL fits against the lattice data points [35–37] and the NLL \oplus NLP LCSR predictions. The available measurements from the BaBar [105, 106], Belle [107–109], LHCb [110, 111] and Belle II Collaborations [112] are also displayed. The red solid and dashed ellipses correspond to 95.45 % and 99.73 % confidence level contours, respectively.

transfer, we will apply the BGL parametrization [29–31] as widely employed in the form-factor determinations (see, for instance [47, 48, 102]) and then perform the binned χ^2 fit of our LCSR predictions at $q^2 \in \{-3.0, -2.0, -1.0, 0.0, 1.0, 2.0\}$ GeV 2 , in combination with the available lattice QCD results. Moreover, we will implement the strong unitarity constraints on the BGL coefficients b_n^i by including all the two-body $\bar{B}_q^{(*)} \rightarrow D_q^{(*)}$ channels. Consequently, we will adopt the HQET relations between these form factors at $\mathcal{O}(\alpha_s, 1/m_b, 1/m_c^2)$, allowing us to express the $\bar{B}_q^* \rightarrow D_q^{(*)}$ form factors in terms of the corresponding $\bar{B}_q \rightarrow D_q^{(*)}$ form factors, the NLP IW functions $\hat{\chi}_{2,3}^{(q)}(\omega)$ and $\hat{\eta}^{(q)}(\omega)$ [103], and the $\mathcal{O}(1/m_c^2)$ IW functions $\hat{\ell}_{1,\dots,6}(\omega)$ [104]. The determined intervals of the normalization and the slop parameters of these IW functions from [50] will therefore be employed.

Combining the obtained LCSR results for the $\bar{B}_q \rightarrow D_q^*$ form factors with I) the updated SCET sum rules for the $\bar{B}_q \rightarrow D_q$ form factors [44], II) the lattice results for the $\bar{B} \rightarrow D$ form factors at $\omega = \{1.00, 1.08, 1.16\}$ from the FNAL/MILC Collaboration [35] and the synthetic data points at $\omega = \{1.01, 1.06\}$ from the HPQCD analysis [36], III) the unquenched lattice results for the $\bar{B} \rightarrow D^*$ form factors at $\omega = \{1.03, 1.10, 1.17\}$ from the FNAL/MILC Collaboration [37], IV) the lattice determinations of the $\bar{B}_s \rightarrow D_s$ form factors at $\omega = \{1.0, 1.06, 1.12\}$ from the HPQCD analysis [39], V) the lattice computations of the $\bar{B}_s \rightarrow D_s^*$ form factors at $\omega = \{1.0, 1.04, 1.08\}$ [40], we display in Table I the resulting z -series coefficients from the combined BGL fitting with the truncation $n = 3$. In order to better understand the phenomenological significance of including

the LCSR data points in the constrained BGL fit, we further carry out an alternative fit to the “only lattice QCD” data points of the $\bar{B} \rightarrow D^{(*)}$ form factors [35–37] and the $\bar{B}_s \rightarrow D_s^{(*)}$ form factors [39, 40]. It needs to be stressed that our major objective is to investigate whether the inclusion of the large-recoil LCSR data points in the BGL fit strategy allows us to increase effectively the precision of the yielding form factors. It is evident from Figure 2 that taking into account the NLL \oplus NLP LCSR results will indeed be highly beneficial for pinning down the uncertainties of the $\bar{B} \rightarrow D^{(*)}$ form factors at small momentum transfer. As the third fit model, we also carry out the statistical analysis by taking into account the experimental data points for $\bar{B}_{(s)} \rightarrow D_{(s)}^{(*)} \ell \bar{\nu}_\ell$ together with the lattice QCD results and the LCSR predictions.

We continue to present the correlated numerical predictions for $\mathcal{R}(D)$ and $\mathcal{R}(D^*)$ in Figure 3, confronting with the available measurements from the BaBar [105, 106], Belle [107–109], LHCb [110, 111] and Belle II Collaborations [112]. Importantly, our determinations of $\mathcal{R}(D)$ and $\mathcal{R}(D^*)$ by encompassing the LCSR results in the numerical fit deviate from the HFLAV-averaged measurements by approximately 2.6σ , in contrast with the 3.3σ discrepancy between the arithmetic average of the previous SM predictions [48, 49, 113] and the state-of-the-art experimental average [13]. Subsequently, we carry out the simultaneous fit for $|V_{cb}|$ and $|V_{ub}|$ by taking the determined $\bar{B}_{(s)} \rightarrow D_{(s)}^{(*)}$ form factors and the updated predictions of the $\bar{B} \rightarrow \pi$ form factors in [46] in combination with the lattice data points for the $\bar{B}_{(s)} \rightarrow D_{(s)}^{(*)}$ form factors [35–37, 39, 40] and for the $\bar{B} \rightarrow \pi$ form factors [114–116] and the experimental measurements for $\bar{B}_{(s)} \rightarrow D_{(s)}^{(*)} \ell \bar{\nu}_\ell$ [1, 3–5] and for $\bar{B} \rightarrow \pi \ell \bar{\nu}_\ell$ [117–121]. The yielding intervals of $|V_{cb}|$ and $|V_{ub}|$ are

$$\{|V_{cb}|, |V_{ub}|\} = \{(39.64 \pm 0.63), (3.71 \pm 0.13)\} \times 10^{-3}, \quad (6)$$

which coincide with the previous exclusive extractions for $|V_{cb}|$ (for instance, [47–53, 122–126]) and for $|V_{ub}|$ (e.g., [91, 127–129]). Unsurprisingly, the obtained numerical predictions (6) remain to be in tension with the world averages of the inclusive determinations $|V_{cb}| = (42.2 \pm 0.8) \times 10^{-3}$ and $|V_{ub}| = (4.13 \pm 0.12^{+0.13}_{-0.14} \pm 0.18) \times 10^{-3}$ [130] at the level of 2.5σ and 1.5σ , respectively. In an attempt to understand qualitatively the systematic uncertainties due to the truncated BGL expansions, we increase the expansion order to $n = 4$ and repeat the numerical fit procedure for the form factors, yielding the theory predictions for both the LFU ratios $\mathcal{R}(D^{(*)})$ and the CKM matrix elements $|V_{cb}|$ and $|V_{ub}|$ only marginally different from the achieved results with $n = 3$.

CONCLUSIONS

In conclusion, we have endeavored to accomplish for the first time the complete next-to-leading-order QCD computations of the $\bar{B}_q \rightarrow D_q^{(*)} \ell \bar{\nu}_\ell$ form factors at large recoil and identified explicitly the unsuppressed charm-quark-mass dependent contributions in the heavy quark expansion. Taking into account the obtained LCSR data points in the BGL z -series fit of the $\bar{B}_q \rightarrow D_q^{(*)} \ell \bar{\nu}_\ell$ form factors enabled us to enhance significantly the achieved accuracy of the large-recoil theory predictions for the $\bar{B} \rightarrow D^{(*)}$ form factors. Implementing the determined LCSR results in the statistical analysis turned out to be advantageous to mitigate the combined $\mathcal{R}(D)$ and $\mathcal{R}(D^*)$ tension between the SM predictions and the HFLAV-averaged measurements. Our computations of the heavy-to-heavy form factors near the maximal recoil will be of notable importance for obtaining the yet higher precision predictions of the $\bar{B}_q \rightarrow D_q^{(*)} \ell \bar{\nu}_\ell$ decay observables, when combined with the upcoming lattice determinations of the bottom-meson distribution amplitudes.

ACKNOWLEDGEMENTS

We are grateful to Thomas Mannel, Zi-Hao Mi, Ru-Ying Tang, Alejandro Vaquero, Chao Wang and Yan-Bing Wei for illuminating discussions. Y.M.W. acknowledges support from the National Natural Science Foundation of China with Grant No. 11735010 and 12075125, and the Natural Science Foundation of Tianjin with Grant No. 19JCJQJC61100.

* boyancui@nankai.edu.cn

† huangyongkang@mail.nankai.edu.cn

‡ correspondence author: wangyuming@nankai.edu.cn

§ correspondence author: zxc@mail.nankai.edu.cn

- [1] R. Glattauer *et al.* (Belle), Phys. Rev. D **93**, 032006 (2016), arXiv:1510.03657 [hep-ex].
- [2] A. Abdesselam *et al.* (Belle), (2017), arXiv:1702.01521 [hep-ex].
- [3] E. Waheed *et al.* (Belle), Phys. Rev. D **100**, 052007 (2019), [Erratum: Phys.Rev.D 103, 079901 (2021)], arXiv:1809.03290 [hep-ex].
- [4] R. Aaij *et al.* (LHCb), Phys. Rev. D **101**, 072004 (2020), arXiv:2001.03225 [hep-ex].
- [5] R. Aaij *et al.* (LHCb), JHEP **12**, 144 (2020), arXiv:2003.08453 [hep-ex].
- [6] M. T. Prim *et al.* (Belle), (2023), arXiv:2301.07529 [hep-ex].
- [7] W. Altmannshofer *et al.* (Belle-II), PTEP **2019**, 123C01 (2019), [Erratum: PTEP 2020, 029201 (2020)], arXiv:1808.10567 [hep-ex].
- [8] P. Gambino *et al.*, Eur. Phys. J. C **80**, 966 (2020), arXiv:2006.07287 [hep-ph].

- [9] P. A. Boyle *et al.*, in *2022 Snowmass Summer Study* (2022) arXiv:2205.15373 [hep-lat].
- [10] A. S. Kronfeld *et al.* (USQCD), (2022), arXiv:2207.07641 [hep-lat].
- [11] A. Di Canto and S. Meinel, (2022), arXiv:2208.05403 [hep-ex].
- [12] F. U. Bernlochner, M. F. Sevilla, D. J. Robinson, and G. Wormser, Rev. Mod. Phys. **94**, 015003 (2022), arXiv:2101.08326 [hep-ex].
- [13] Y. Amhis *et al.* (HFLAV), (2022), arXiv:2206.07501 [hep-ex].
- [14] F. U. Bernlochner and Z. Ligeti, Phys. Rev. D **95**, 014022 (2017), arXiv:1606.09300 [hep-ph].
- [15] F. U. Bernlochner, Z. Ligeti, D. J. Robinson, and W. L. Sutcliffe, Phys. Rev. Lett. **121**, 202001 (2018), arXiv:1808.09464 [hep-ph].
- [16] T. D. Cohen, H. Lamm, and R. F. Lebed, Phys. Rev. D **98**, 034022 (2018), arXiv:1807.00256 [hep-ph].
- [17] N. Das and R. Dutta, Phys. Rev. D **105**, 055027 (2022), arXiv:2110.05526 [hep-ph].
- [18] N. Gubernari, A. Khodjamirian, R. Mandal, and T. Mannel, JHEP **05**, 029 (2022), arXiv:2203.08493 [hep-ph].
- [19] F. U. Bernlochner, Z. Ligeti, M. Papucci, and D. J. Robinson, Phys. Rev. D **107**, L011502 (2023), arXiv:2206.11282 [hep-ph].
- [20] S. Patnaik and R. Singh, Universe **9**, 129 (2023), arXiv:2211.04348 [hep-ph].
- [21] S. Patnaik, L. Nayak, and R. Singh, (2023), arXiv:2308.05677 [hep-ph].
- [22] N. Penalva, J. M. Flynn, E. Hernández, and J. Nieves, (2023), arXiv:2304.00250 [hep-ph].
- [23] R. Aaij *et al.* (LHCb), (2022), arXiv:2212.09152 [hep-ex].
- [24] R. Aaij *et al.* (LHCb), (2022), arXiv:2212.09153 [hep-ex].
- [25] N. R. Singh Chundawat, Phys. Rev. D **107**, 055004 (2023), arXiv:2212.01229 [hep-ph].
- [26] A. K. Alok, N. R. Singh Chundawat, and A. Mandal, (2023), arXiv:2303.16606 [hep-ph].
- [27] M. Algueró, A. Biswas, B. Capdevila, S. Descotes-Genon, J. Matias, and M. Novoa-Brunet, Eur. Phys. J. C **83**, 648 (2023), arXiv:2304.07330 [hep-ph].
- [28] R. Fleischer, E. Malami, A. Rehult, and K. K. Vos, JHEP **06**, 033 (2023), arXiv:2303.08764 [hep-ph].
- [29] C. G. Boyd, B. Grinstein, and R. F. Lebed, Phys. Lett. B **353**, 306 (1995), arXiv:hep-ph/9504235.
- [30] C. G. Boyd, B. Grinstein, and R. F. Lebed, Nucl. Phys. B **461**, 493 (1996), arXiv:hep-ph/9508211.
- [31] C. G. Boyd, B. Grinstein, and R. F. Lebed, Phys. Rev. D **56**, 6895 (1997), arXiv:hep-ph/9705252.
- [32] I. Caprini and C. Macesanu, Phys. Rev. D **54**, 5686 (1996), arXiv:hep-ph/9605365.
- [33] I. Caprini, L. Lellouch, and M. Neubert, Nucl. Phys. B **530**, 153 (1998), arXiv:hep-ph/9712417.
- [34] C. Bourrely, I. Caprini, and L. Lellouch, Phys. Rev. D **79**, 013008 (2009), [Erratum: Phys.Rev.D 82, 099902 (2010)], arXiv:0807.2722 [hep-ph].
- [35] J. A. Bailey *et al.* (MILC), Phys. Rev. D **92**, 034506 (2015), arXiv:1503.07237 [hep-lat].
- [36] H. Na, C. M. Bouchard, G. P. Lepage, C. Monahan, and J. Shigemitsu (HPQCD), Phys. Rev. D **92**, 054510 (2015), [Erratum: Phys.Rev.D 93, 119906 (2016)], arXiv:1505.03925 [hep-lat].

- [37] A. Bazavov *et al.* (Fermilab Lattice, MILC), Eur. Phys. J. C **82**, 1141 (2022), arXiv:2105.14019 [hep-lat].
- [38] J. A. Bailey *et al.*, Phys. Rev. D **85**, 114502 (2012), [Erratum: Phys. Rev. D 86, 039904 (2012)], arXiv:1202.6346 [hep-lat].
- [39] E. McLean, C. T. H. Davies, J. Koponen, and A. T. Lytle, Phys. Rev. D **101**, 074513 (2020), arXiv:1906.00701 [hep-lat].
- [40] J. Harrison and C. T. H. Davies (HPQCD), Phys. Rev. D **105**, 094506 (2022), arXiv:2105.11433 [hep-lat].
- [41] S. Faller, A. Khodjamirian, C. Klein, and T. Mannel, Eur. Phys. J. C **60**, 603 (2009), arXiv:0809.0222 [hep-ph].
- [42] N. Gubernari, A. Kokulu, and D. van Dyk, JHEP **01**, 150 (2019), arXiv:1811.00983 [hep-ph].
- [43] Y.-M. Wang, Y.-B. Wei, Y.-L. Shen, and C.-D. Lü, JHEP **06**, 062 (2017), arXiv:1701.06810 [hep-ph].
- [44] J. Gao, T. Huber, Y. Ji, C. Wang, Y.-M. Wang, and Y.-B. Wei, JHEP **05**, 024 (2022), arXiv:2112.12674 [hep-ph].
- [45] M. C. Arnesen, B. Grinstein, I. Z. Rothstein, and I. W. Stewart, Phys. Rev. Lett. **95**, 071802 (2005), arXiv:hep-ph/0504209.
- [46] B.-Y. Cui, Y.-K. Huang, Y.-L. Shen, C. Wang, and Y.-M. Wang, JHEP **03**, 140 (2023), arXiv:2212.11624 [hep-ph].
- [47] D. Bigi, P. Gambino, and S. Schacht, JHEP **11**, 061 (2017), arXiv:1707.09509 [hep-ph].
- [48] P. Gambino, M. Jung, and S. Schacht, Phys. Lett. B **795**, 386 (2019), arXiv:1905.08209 [hep-ph].
- [49] M. Bordone, M. Jung, and D. van Dyk, Eur. Phys. J. C **80**, 74 (2020), arXiv:1908.09398 [hep-ph].
- [50] M. Bordone, N. Gubernari, D. van Dyk, and M. Jung, Eur. Phys. J. C **80**, 347 (2020), arXiv:1912.09335 [hep-ph].
- [51] S. Jaiswal, S. Nandi, and S. K. Patra, JHEP **12**, 060 (2017), arXiv:1707.09977 [hep-ph].
- [52] S. Jaiswal, S. Nandi, and S. K. Patra, JHEP **06**, 165 (2020), arXiv:2002.05726 [hep-ph].
- [53] A. Biswas, S. Nandi, and I. Ray, (2022), arXiv:2212.02528 [hep-ph].
- [54] K. Cheung, Z.-R. Huang, H.-D. Li, C.-D. Lü, Y.-N. Mao, and R.-Y. Tang, Nucl. Phys. B **965**, 115354 (2021), arXiv:2002.07272 [hep-ph].
- [55] H. Boos, T. Feldmann, T. Mannel, and B. D. Pecjak, Phys. Rev. D **73**, 036003 (2006), arXiv:hep-ph/0504005.
- [56] H. Boos, T. Feldmann, T. Mannel, and B. D. Pecjak, JHEP **05**, 056 (2006), arXiv:hep-ph/0512157.
- [57] J. Gao, C.-D. Lü, Y.-L. Shen, Y.-M. Wang, and Y.-B. Wei, Phys. Rev. D **101**, 074035 (2020), arXiv:1907.11092 [hep-ph].
- [58] M. Beneke and D. Yang, Nucl. Phys. B **736**, 34 (2006), arXiv:hep-ph/0508250.
- [59] M. Beneke, Y. Kiyo, and D. s. Yang, Nucl. Phys. B **692**, 232 (2004), arXiv:hep-ph/0402241.
- [60] R. J. Hill, T. Becher, S. J. Lee, and M. Neubert, JHEP **07**, 081 (2004), arXiv:hep-ph/0404217.
- [61] F. De Fazio, T. Feldmann, and T. Hurth, Nucl. Phys. B **733**, 1 (2006), [Erratum: Nucl. Phys. B 800, 405 (2008)], arXiv:hep-ph/0504088.
- [62] F. De Fazio, T. Feldmann, and T. Hurth, JHEP **02**, 031 (2008), arXiv:0711.3999 [hep-ph].
- [63] A. Khodjamirian, T. Mannel, and N. Offen, Phys. Lett. B **620**, 52 (2005), arXiv:hep-ph/0504091.
- [64] A. Khodjamirian, T. Mannel, and N. Offen, Phys. Rev. D **75**, 054013 (2007), arXiv:hep-ph/0611193.
- [65] M. Beneke and T. Feldmann, Phys. Lett. B **553**, 267 (2003), arXiv:hep-ph/0211358.
- [66] A. K. Leibovich, Z. Ligeti, and M. B. Wise, Phys. Lett. B **564**, 231 (2003), arXiv:hep-ph/0303099.
- [67] P. Böer, *QCD Factorisation in Exclusive Semileptonic B Decays: New Applications and Resummation of Rapidity Logarithms*, Ph.D. thesis, University of Siegen, <https://dspace.ub.uni-siegen.de/handle/ubsi/1369>, (2018).
- [68] B. Geyer and O. Witzel, Phys. Rev. D **72**, 034023 (2005), arXiv:hep-ph/0502239.
- [69] V. M. Braun, Y. Ji, and A. N. Manashov, JHEP **05**, 022 (2017), arXiv:1703.02446 [hep-ph].
- [70] M. Beneke, V. M. Braun, Y. Ji, and Y.-B. Wei, JHEP **07**, 154 (2018), arXiv:1804.04962 [hep-ph].
- [71] G. Bell, T. Feldmann, Y.-M. Wang, and M. W. Y. Yip, JHEP **11**, 191 (2013), arXiv:1308.6114 [hep-ph].
- [72] Y.-M. Wang and Y.-L. Shen, Nucl. Phys. B **898**, 563 (2015), arXiv:1506.00667 [hep-ph].
- [73] Y.-M. Wang, JHEP **09**, 159 (2016), arXiv:1606.03080 [hep-ph].
- [74] Y.-M. Wang and Y.-L. Shen, JHEP **05**, 184 (2018), arXiv:1803.06667 [hep-ph].
- [75] Y.-L. Shen, Y.-M. Wang, and Y.-B. Wei, JHEP **12**, 169 (2020), arXiv:2009.02723 [hep-ph].
- [76] C. Wang, Y.-M. Wang, and Y.-B. Wei, JHEP **02**, 141 (2022), arXiv:2111.11811 [hep-ph].
- [77] T. Feldmann, P. Lüghausen, and D. van Dyk, JHEP **10**, 162 (2022), arXiv:2203.15679 [hep-ph].
- [78] V. M. Braun, D. Y. Ivanov, and G. P. Korchemsky, Phys. Rev. D **69**, 034014 (2004), arXiv:hep-ph/0309330.
- [79] A. Khodjamirian, R. Mandal, and T. Mannel, JHEP **10**, 043 (2020), arXiv:2008.03935 [hep-ph].
- [80] A. G. Grozin and M. Neubert, Phys. Rev. D **55**, 272 (1997), arXiv:hep-ph/9607366.
- [81] T. Nishikawa and K. Tanaka, Nucl. Phys. B **879**, 110 (2014), arXiv:1109.6786 [hep-ph].
- [82] M. Rahimi and M. Wald, Phys. Rev. D **104**, 016027 (2023), arXiv:2012.12165 [hep-ph].
- [83] W. Wang, Y.-M. Wang, J. Xu, and S. Zhao, Phys. Rev. D **102**, 011502 (2020), arXiv:1908.09933 [hep-ph].
- [84] Y. Aoki *et al.* (Flavour Lattice Averaging Group (FLAG)), Eur. Phys. J. C **82**, 869 (2022), arXiv:2111.09849 [hep-lat].
- [85] B. Pullin and R. Zwicky, JHEP **09**, 023 (2021), arXiv:2106.13617 [hep-ph].
- [86] A. Khodjamirian, C. Klein, T. Mannel, and N. Offen, Phys. Rev. D **80**, 114005 (2009), arXiv:0907.2842 [hep-ph].
- [87] G. Duplancic and B. Melic, JHEP **11**, 138 (2015), arXiv:1508.05287 [hep-ph].
- [88] H.-D. Li, C.-D. Lü, C. Wang, Y.-M. Wang, and Y.-B. Wei, JHEP **04**, 023 (2020), arXiv:2002.03825 [hep-ph].
- [89] A. Khodjamirian, B. Melić, Y.-M. Wang, and Y.-B. Wei, JHEP **03**, 016 (2021), arXiv:2011.11275 [hep-ph].
- [90] I. Sentitemsu Imsong, A. Khodjamirian, T. Mannel, and D. van Dyk, JHEP **02**, 126 (2015), arXiv:1409.7816 [hep-ph].
- [91] D. Leljak, B. Melić, and D. van Dyk, JHEP **07**, 036 (2021), arXiv:2102.07233 [hep-ph].
- [92] B. Chibisov, R. D. Dikeman, M. A. Shifman, and N. Uraltsev, Int. J. Mod. Phys. A **12**, 2075 (1997),

- arXiv:hep-ph/9605465.
- [93] M. A. Shifman, in *8th International Symposium on Heavy Flavor Physics*, Vol. 3 (World Scientific, Singapore, 2000) pp. 1447–1494, arXiv:hep-ph/0009131.
- [94] I. I. Y. Bigi and N. Uraltsev, Int. J. Mod. Phys. A **16**, 5201 (2001), arXiv:hep-ph/0106346.
- [95] O. Cata, M. Golterman, and S. Peris, JHEP **08**, 076 (2005), arXiv:hep-ph/0506004.
- [96] M. Beylich, G. Buchalla, and T. Feldmann, Eur. Phys. J. C **71**, 1635 (2011), arXiv:1101.5118 [hep-ph].
- [97] M. Jamin, JHEP **09**, 141 (2011), arXiv:1103.2718 [hep-ph].
- [98] J. Dingfelder and T. Mannel, Rev. Mod. Phys. **88**, 035008 (2016).
- [99] D. Boito, I. Caprini, M. Golterman, K. Maltman, and S. Peris, Phys. Rev. D **97**, 054007 (2018), arXiv:1711.10316 [hep-ph].
- [100] A. Pich, Prog. Part. Nucl. Phys. **117**, 103846 (2021), arXiv:2012.04716 [hep-ph].
- [101] A. Pich and A. Rodríguez-Sánchez, JHEP **07**, 145 (2022), arXiv:2205.07587 [hep-ph].
- [102] D. Bigi, P. Gambino, and S. Schacht, Phys. Lett. B **769**, 441 (2017), arXiv:1703.06124 [hep-ph].
- [103] M. Neubert, Phys. Rept. **245**, 259 (1994), arXiv:hep-ph/9306320.
- [104] A. F. Falk and M. Neubert, Phys. Rev. D **47**, 2965 (1993), arXiv:hep-ph/9209268.
- [105] J. P. Lees *et al.* (BaBar), Phys. Rev. Lett. **109**, 101802 (2012), arXiv:1205.5442 [hep-ex].
- [106] J. P. Lees *et al.* (BaBar), Phys. Rev. D **88**, 072012 (2013), arXiv:1303.0571 [hep-ex].
- [107] M. Huschle *et al.* (Belle), Phys. Rev. D **92**, 072014 (2015), arXiv:1507.03233 [hep-ex].
- [108] G. Caria *et al.* (Belle), Phys. Rev. Lett. **124**, 161803 (2020), arXiv:1910.05864 [hep-ex].
- [109] S. Hirose *et al.* (Belle), Phys. Rev. Lett. **118**, 211801 (2017), arXiv:1612.00529 [hep-ex].
- [110] R. Aaij *et al.* (LHCb), (2023), arXiv:2302.02886 [hep-ex].
- [111] R. Aaij *et al.* (LHCb), (2023), arXiv:2305.01463 [hep-ex].
- [112] K. Kojima *et al.* (Belle II), Talk presented at the Lepton Photon Conference (2023).
- [113] D. Bigi and P. Gambino, Phys. Rev. D **94**, 094008 (2016), arXiv:1606.08030 [hep-ph].
- [114] J. M. Flynn, T. Izubuchi, T. Kawanai, C. Lehner, A. Soni, R. S. Van de Water, and O. Witzel, Phys. Rev. D **91**, 074510 (2015), arXiv:1501.05373 [hep-lat].
- [115] J. A. Bailey *et al.* (Fermilab Lattice, MILC), Phys. Rev. D **92**, 014024 (2015), arXiv:1503.07839 [hep-lat].
- [116] J. A. Bailey *et al.* (Fermilab Lattice, MILC), Phys. Rev. Lett. **115**, 152002 (2015), arXiv:1507.01618 [hep-ph].
- [117] P. del Amo Sanchez *et al.* (BaBar), Phys. Rev. D **83**, 032007 (2011), arXiv:1005.3288 [hep-ex].
- [118] J. P. Lees *et al.* (BaBar), Phys. Rev. D **86**, 092004 (2012), arXiv:1208.1253 [hep-ex].
- [119] H. Ha *et al.* (Belle), Phys. Rev. D **83**, 071101 (2011), arXiv:1012.0090 [hep-ex].
- [120] A. Sibidanov *et al.* (Belle), Phys. Rev. D **88**, 032005 (2013), arXiv:1306.2781 [hep-ex].
- [121] K. Adamczyk *et al.* (Belle-II), (2022), arXiv:2210.04224 [hep-ex].
- [122] B. Grinstein and A. Kobach, Phys. Lett. B **771**, 359 (2017), arXiv:1703.08170 [hep-ph].
- [123] G. Martinelli, S. Simula, and L. Vittorio, Phys. Rev. D **105**, 034503 (2022), arXiv:2105.08674 [hep-ph].
- [124] G. Martinelli, S. Simula, and L. Vittorio, Eur. Phys. J. C **82**, 1083 (2022), arXiv:2109.15248 [hep-ph].
- [125] G. Martinelli, M. Naviglio, S. Simula, and L. Vittorio, Phys. Rev. D **106**, 093002 (2022), arXiv:2204.05925 [hep-ph].
- [126] S. Iguro and R. Watanabe, JHEP **08**, 006 (2020), arXiv:2004.10208 [hep-ph].
- [127] A. Biswas, S. Nandi, S. K. Patra, and I. Ray, JHEP **07**, 082 (2021), arXiv:2103.01809 [hep-ph].
- [128] A. Biswas and S. Nandi, JHEP **09**, 127 (2021), arXiv:2105.01732 [hep-ph].
- [129] G. Martinelli, S. Simula, and L. Vittorio, JHEP **08**, 022 (2022), arXiv:2202.10285 [hep-ph].
- [130] R. L. Workman *et al.* (Particle Data Group), PTEP **2022**, 083C01 (2022).
- [131] M. Beneke and T. Feldmann, Nucl. Phys. B **592**, 3 (2001), arXiv:hep-ph/0008255.
- [132] Y.-M. Wang and Y.-L. Shen, JHEP **02**, 179 (2016), arXiv:1511.09036 [hep-ph].
- [133] M. Beneke, A. Maier, J. Piclum, and T. Rauh, Nucl. Phys. B **891**, 42 (2015), arXiv:1411.3132 [hep-ph].
- [134] M. Beneke, C. Bobeth, and Y.-M. Wang, JHEP **12**, 148 (2020), arXiv:2008.12494 [hep-ph].
- [135] V. M. Belyaev, A. Khodjamirian, and R. Rückl, Z. Phys. C **60**, 349 (1993), arXiv:hep-ph/9305348.
- [136] A. Ali, V. M. Braun, and H. Simma, Z. Phys. C **63**, 437 (1994), arXiv:hep-ph/9401277.
- [137] P. Ball and V. M. Braun, Phys. Rev. D **55**, 5561 (1997), arXiv:hep-ph/9701238.
- [138] G. Duplancic, A. Khodjamirian, T. Mannel, B. Melic, and N. Offen, JHEP **04**, 014 (2008), arXiv:0801.1796 [hep-ph].
- [139] A. Khodjamirian, T. Mannel, N. Offen, and Y. M. Wang, Phys. Rev. D **83**, 094031 (2011), arXiv:1103.2655 [hep-ph].
- [140] P. Colangelo and A. Khodjamirian, At the Frontier of Particle Physics / Handbook of QCD **3**, 1495 (2000), arXiv:hep-ph/0010175.

SUPPLEMENTAL MATERIAL

Analytic Expressions for the SCET Form Factors

We first provide explicitly the conversion relations between the helicity form factors $\{\mathcal{V}, \mathcal{A}_0, \mathcal{A}_1, \mathcal{A}_{12}\}$ and the conventional form-factor basis $\{V, A_0, A_1, A_2\}$ (see, for instance [131])

$$\mathcal{V} = \frac{m_{B_q}}{m_{B_q} + m_{D_q^*}} V, \quad \mathcal{A}_0 = \frac{2 m_{D_q^*}}{n \cdot p} A_0, \quad \mathcal{A}_1 = \frac{m_B + m_{D_q^*}}{n \cdot p} A_1, \quad \mathcal{A}_{12} = \mathcal{A}_1 - \frac{m_B - m_{D_q^*}}{m_B} A_2. \quad (7)$$

We then collect the analytic expressions for the hard matching coefficients in the SCET_I representations of the semileptonic $\bar{B}_q \rightarrow D_q^*$ form factors at large hadronic recoil

$$\begin{aligned} C_{f+}^{(A0)} &= 1 + \frac{\alpha_s C_F}{4\pi} \left[-2 \ln^2 \left(\frac{r}{\hat{\mu}} \right) + 5 \ln \left(\frac{r}{\hat{\mu}} \right) - 2 \text{Li}_2(1-r) - 3 \ln r - \frac{\pi^2}{12} - 6 \right] + \mathcal{O}(\alpha_s^2), \\ C_{f0}^{(A0)} &= 1 + \frac{\alpha_s C_F}{4\pi} \left[-2 \ln^2 \left(\frac{r}{\hat{\mu}} \right) + 5 \ln \left(\frac{r}{\hat{\mu}} \right) - 2 \text{Li}_2(1-r) - \frac{3-5r}{1-r} \ln r - \frac{\pi^2}{12} - 4 \right] + \mathcal{O}(\alpha_s^2), \\ C_V^{(A0)} &= 1 + \frac{\alpha_s C_F}{4\pi} \left[-2 \ln^2 \left(\frac{r}{\hat{\mu}} \right) + 5 \ln \left(\frac{r}{\hat{\mu}} \right) - 2 \text{Li}_2(1-r) - \frac{3-2r}{1-r} \ln r - \frac{\pi^2}{12} - 6 \right] + \mathcal{O}(\alpha_s^2), \\ C_{f+}^{(A1, m_c)} &= (r-1) + \mathcal{O}(\alpha_s), \quad C_{f0}^{(A1, m_c)} = (1-r) + \mathcal{O}(\alpha_s), \quad C_V^{(A1, m_c)} = -1 + \mathcal{O}(\alpha_s), \quad C_{A_1}^{(A1, m_c)} = 1 + \mathcal{O}(\alpha_s), \\ C_{f+}^{(B1)} &= \left(-2 + \frac{1}{r} \right) + \mathcal{O}(\alpha_s), \quad C_{f0}^{(B1)} = \left(-\frac{1}{r} \right) + \mathcal{O}(\alpha_s), \quad C_V^{(B1)} = 0 + \mathcal{O}(\alpha_s), \end{aligned} \quad (8)$$

with the two dimensionless quantities $r = n \cdot p / m_b$ and $\hat{\mu} = \mu / m_b$.

We present further the effective Lagrangian densities $\mathcal{L}_{\xi m_c}^{(0)}$ and $\mathcal{L}_{\xi q, m_q}^{(2)}$ together with the SCET_I weak current $O_{\parallel}^{(A0)}$ entering the SCET correlation function $\Pi_{\nu, \parallel}^{(A0)}$

$$\begin{aligned} \mathcal{L}_{\xi m_c}^{(0)} &= m_c \bar{\xi} \left[i \not{D}_{\perp c}, \frac{1}{in \cdot D_c} \right] \frac{\not{p}}{2} \xi - m_c^2 \bar{\xi} \frac{1}{in \cdot D_c} \frac{\not{p}}{2} \xi, \\ \mathcal{L}_{\xi q, m_q}^{(2)} &= -m_q \left[(\bar{\xi} W_c) (Y_s^\dagger q_s) + (\bar{q}_s Y_s) (W_c^\dagger \xi) \right], \\ O_{\parallel}^{(A0)} &= (\bar{\xi} W_c) \gamma_5 h_v, \end{aligned} \quad (9)$$

which are evidently in demand for the construction of the SCET sum rules (5) for the effective form factor ξ_{\parallel} in the main text. The sample Feynman diagrams for the one-loop computation of the correction function $\Pi_{\nu, \parallel}^{(A0)}$ with the aid of the perturbative factorization technique are collected in (a), (b) and (c) in Figure 4. In particular, the three effective bottom-meson distribution amplitudes $\phi_{B, \text{eff}}^-$, $\phi_{B, \text{eff}}^{+, m_c}$ and $\phi_{B, \text{eff}}^{+, m_q}$ in the NLO sum rules for the SCET form factor ξ_{\parallel} can be written as

$$\begin{aligned} \phi_{B, \text{eff}}^-(\omega') &= \theta(\omega' - \omega_c) \phi_B^-(\omega' - \omega_c) + \frac{\alpha_s C_F}{4\pi} \left\{ \int_0^\infty d\omega [\theta(\omega' - \omega - \omega_c) \varrho_1(\omega, \omega') + \theta(\omega + \omega_c - \omega') \varrho_2(\omega, \omega')] \frac{d}{d\omega} \phi_B^-(\omega) \right. \\ &\quad \left. + \int_0^\infty d\omega \varrho_3(\omega, \omega') \phi_B^-(\omega) - 4\omega_c \left[3 \ln \frac{\mu}{m_c} + 2 \right] \frac{d}{d\omega'} [\phi_B^-(\omega' - \omega_c) \theta(\omega' - \omega_c)] \right\} + \mathcal{O}(\alpha_s^2), \\ \phi_{B, \text{eff}}^{+, m_c}(\omega') &= -\frac{\alpha_s C_F}{4\pi} \theta(\omega' - \omega_c) \int_0^\infty d\omega [\theta(\omega' - \omega - \omega_c) \varrho_4(\omega, \omega') + \theta(\omega + \omega_c - \omega') \varrho_5(\omega, \omega')] \frac{d}{d\omega} \frac{\phi_B^+(\omega)}{\omega} + \mathcal{O}(\alpha_s^2), \\ \phi_{B, \text{eff}}^{+, m_q}(\omega') &= \frac{\alpha_s C_F}{4\pi} \theta(\omega' - \omega_c) \left\{ \int_0^\infty d\omega [\theta(\omega' - \omega - \omega_c) \varrho_6(\omega, \omega') + \theta(\omega + \omega_c - \omega') \varrho_7(\omega, \omega')] \frac{d}{d\omega} \frac{\phi_B^+(\omega)}{\omega} \right. \\ &\quad \left. + \int_0^\infty d\omega [\theta(\omega' - \omega - \omega_c) \varrho_8(\omega, \omega') + \theta(\omega + \omega_c - \omega') \varrho_9(\omega, \omega')] \frac{\phi_B^+(\omega)}{\omega^2} \right\} + \mathcal{O}(\alpha_s^2), \end{aligned} \quad (10)$$

where we have introduced the new coefficient functions ϱ_i (with $i = 1, \dots, 9$) for convenience

$$\varrho_1(\omega, \omega') = \ln \frac{\omega' - \omega - \omega_c}{\omega' - \omega_c} \left[\left(1 - \frac{\omega_c}{\omega'} \right)^2 - 4 \ln \frac{\omega_c}{\omega' - \omega - \omega_c} - 2 \ln \frac{\mu^2}{n \cdot p \omega'} - 2 \right],$$

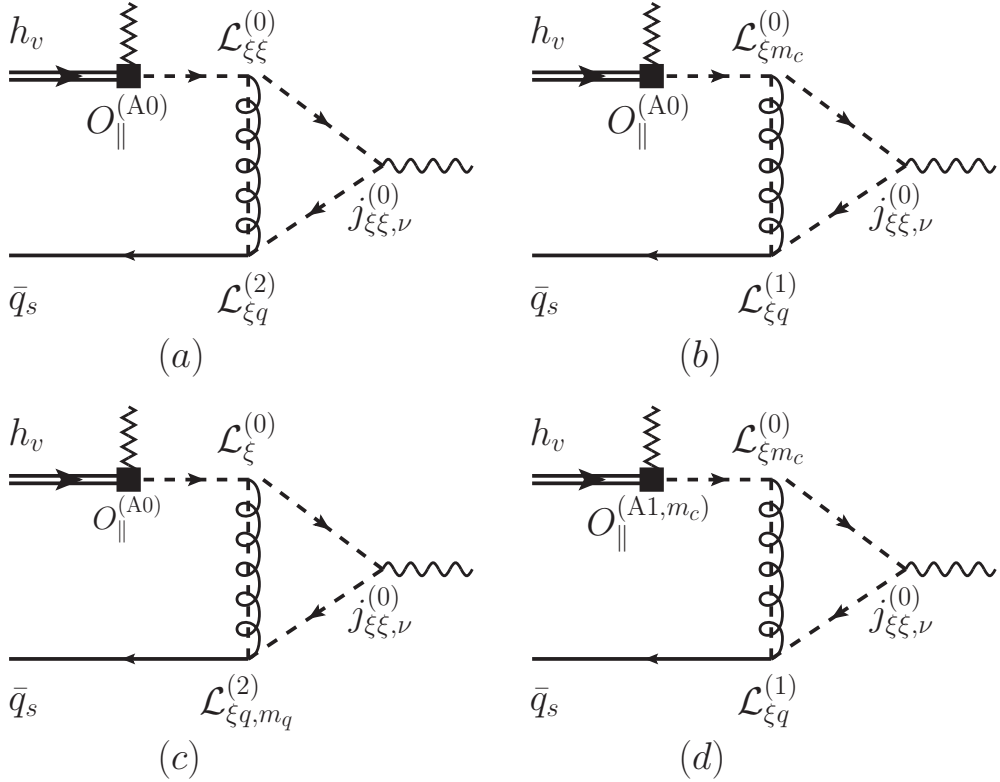


FIG. 4. Sample diagrams for the two bottom-meson-to-vacuum correlation functions $\Pi_{\nu, \parallel}^{(A0)}$ and $\Pi_{\nu, \parallel}^{(A1), m_c}$ in SCET_I.

$$\begin{aligned}
\varrho_2(\omega, \omega') &= \ln \frac{\omega + \omega_c - \omega'}{\omega' - \omega_c} \left[\left(1 - \frac{\omega_c}{\omega'}\right)^2 + 4 \ln \frac{\mu}{\omega' - \omega_c} + 2 \ln \frac{\omega'}{n \cdot p} + 2 \right] + 2 \text{Li}_2 \left(\frac{\omega_c}{\omega_c - \omega'} \right) \\
&\quad + \ln \frac{\omega_c}{\omega' - \omega_c} \left[\left(1 - \frac{\omega_c}{\omega'}\right)^2 - 2 \ln \frac{\omega_c}{\omega'} - 2 \right] - \ln^2 \frac{\mu^2}{n \cdot p (\omega' - \omega_c)} - \frac{\omega_c}{\omega'} - \frac{5\pi^2}{6}, \\
\varrho_3(\omega, \omega') &= \theta(\omega' - \omega - \omega_c) \frac{1}{\omega + \omega_c - \omega'} \left[4 \ln \frac{\omega' - \omega}{\omega_c} - \left(\frac{\omega' - \omega - \omega_c}{\omega' - \omega} \right)^2 \right] + \theta(\omega + \omega_c - \omega') \frac{2}{\omega}, \\
\varrho_4(\omega, \omega') &= \frac{(\omega' - \omega_c)^2}{\omega'} \ln \frac{\omega' - \omega - \omega_c}{\omega' - \omega_c} - \omega' \ln \frac{\omega' - \omega}{\omega'} - \frac{\omega \omega_c}{\omega' - \omega}, \\
\varrho_5(\omega, \omega') &= \frac{(\omega' - \omega_c)^2}{\omega'} \ln \frac{(\omega + \omega_c - \omega') \omega_c}{(\omega' - \omega_c)^2} - \omega' \ln \frac{\omega_c}{\omega'}, \\
\varrho_6(\omega, \omega') &= \left[2\omega' + \omega_c \left(1 + \frac{\omega_c}{\omega'} \right) \right] \ln \frac{\omega' - \omega_c}{\omega' - \omega_c - \omega}, \\
\varrho_7(\omega, \omega') &= \left[2\omega' + \omega_c \left(1 + \frac{\omega_c}{\omega'} \right) \right] \ln \frac{(\omega' - \omega_c)^2}{\omega_c (\omega + \omega_c - \omega')} - \left(2 \ln \frac{\mu^2}{m_c^2} + 5 \right) \omega' + \omega_c, \\
\varrho_8(\omega, \omega') &= 2\omega' \left[\ln \frac{\omega' - \omega}{\omega'} + 2 \ln \frac{\omega' - \omega_c}{\omega' - \omega_c - \omega} \right] + \frac{\omega \omega_c}{\omega - \omega'}, \\
\varrho_9(\omega, \omega') &= -\omega' \left[4 \ln \frac{\mu}{\omega' - \omega_c} + 2 \ln \frac{\omega'}{n \cdot p} + 5 \right] + \omega_c.
\end{aligned} \tag{11}$$

Along the same vein, we can establish the desired LCSR for the effective form factor ξ_{\parallel, m_c} by employing the bottom-meson-to-vacuum correction function

$$\Pi_{\nu, \parallel}^{(A1, m_c)} = \int d^4x e^{ip \cdot x} \int d^4y \int d^4z \langle 0 | T \{ j_{\xi\xi, \parallel \nu}^{(0)}(x), i\mathcal{L}_{\xi q}^{(1)}(y), i\mathcal{L}_{\xi m_c}^{(0)}(z), O_{\parallel}^{(A1, m_c)}(0) \} | \bar{B}_v \rangle, \tag{12}$$

where the manifest form of the A1-type SCET_I current is given by

$$O_{\parallel}^{(A1, m_c)}(0) = (\bar{\xi}W_c) \frac{\not{q}}{2} \frac{m_c}{-in \cdot \overleftarrow{D}_c} \gamma_5 h_v. \quad (13)$$

It turns out that only the diagram (d) in Figure 4 can yield the non-vanishing contribution to the correlation function (12) at $\mathcal{O}(\alpha_s)$. Equating the obtained partonic representation with the counterpart hadronic dispersion relation allows us to derive the new sum rules for ξ_{\parallel, m_c}

$$\xi_{\parallel, m_c} = 2 \frac{\mathcal{F}_{B_q}(\mu)}{f_{D_q^*, \parallel}} \frac{m_{B_q} m_{D_q^*}}{(n \cdot p)^2} \int_0^{\omega_s} d\omega' \exp \left[\frac{m_{D_q^*}^2 - n \cdot p \omega'}{n \cdot p \omega_M} \right] \left[\frac{\omega_c}{\omega'} \phi_{B, \text{eff}}^{+, m_c}(\omega') \right], \quad (14)$$

with $\omega_c = m_c^2/n \cdot p$. We mention in passing that the default power counting rules for ω_s , ω_M and ω_c are

$$\omega_c \sim \omega_s \sim \mathcal{O}(\Lambda_{\text{QCD}}), \quad (\omega_s - \omega_c) \sim \mathcal{O}(\Lambda_{\text{QCD}}^{3/2}/m_b^{1/2}), \quad \omega_M \sim \mathcal{O}(\Lambda_{\text{QCD}}^{3/2}/m_b^{1/2}), \quad (15)$$

which differ from the conventional counting schemes for the exclusive charmless bottom-hadron decays [72–75, 132].

Now we turn to derive the SCET sum rules for the B1-type longitudinal form factor Ξ_{\parallel} by investigating the bottom-meson-to-vacuum correlation function

$$\Pi_{\nu, \parallel}^{(B1)} = \frac{n \cdot p}{2\pi} \int d^4x e^{ip \cdot x} \int dr e^{-in \cdot p \tau r} \int d^4y \langle 0 | T\{j_{\xi\xi, \parallel\nu}^{(0)}(x), i\mathcal{L}_{\xi q}^{(1)}(y), O_{\parallel}^{(B1)}(rn)\} | \bar{B}_v \rangle, \quad (16)$$

where the non-local effective current $O_{\parallel}^{(B1)}$ reads

$$O_{\parallel}^{(B1)} = (\bar{\xi}W_c)(0) \gamma_5 (W_c^\dagger i\cancel{D}_{c\perp} W_c)(rn) h_v(0). \quad (17)$$

It is then straightforward to construct the one-loop LCSR for the non-local form factor Ξ_{\parallel} with the HQET bottom-meson distribution amplitude [57]

$$\Xi_{\parallel} = -\frac{\alpha_s C_F}{\pi} \frac{\mathcal{F}_{B_q}(\mu)}{f_{D_q^*, \parallel}} \frac{m_{B_q} m_{D_q^*}}{n \cdot p m_b} \bar{\tau} \theta(\tau) \theta\left(\bar{\tau} - \frac{\omega_c}{\omega_s}\right) \int_{\omega_c/\bar{\tau}}^{\omega_s} d\omega' \exp \left[\frac{m_{D_q^*}^2 - n \cdot p \omega'}{n \cdot p \omega_M} \right] \int_{\omega' - \omega_c/\bar{\tau}}^{+\infty} \frac{d\omega}{\omega} \phi_B^+(\omega), \quad (18)$$

with $\bar{\tau} = 1 - \tau$. Adopting the factorization scale of order $\sqrt{m_b \Lambda_{\text{QCD}}}$, we continue to perform the next-to-leading-logarithmic (NLL) resummation for the enhanced logarithms in the final expressions of the considered QCD form factors by employing the standard renormalization-group (RG) formalism (see [44, 46] for further details).

Likewise, we can construct the SCET sum rules for the transverse form factors ξ_{\perp} , ξ_{\perp, m_c} and Ξ_{\perp} by adopting three additional correlation functions $\Pi_{\mu\nu\rho, \perp}^{(A0)}$, $\Pi_{\mu\nu\rho, \perp}^{(A1, m_c)}$ and $\Pi_{\mu\nu\rho, \perp}^{(B1)}$, which can be obtained from the counterpart longitudinal correlation functions $\Pi_{\nu, \parallel}^{(A0)}$, $\Pi_{\nu, \parallel}^{(A1, m_c)}$ and $\Pi_{\nu, \parallel}^{(B1)}$ with the appropriate replacement rules (see [57]).

$$j_{\xi q, \parallel\nu}^{(0,2)} \rightarrow j_{\xi q, \perp\nu\rho}^{(0,2)}, \quad O_{\parallel}^{(A0)} \rightarrow O_{\perp, \mu}^{(A0)}, \quad O_{\parallel}^{(A1, m_c)} \rightarrow O_{\perp, \mu}^{(A1, m_c)}, \quad O_{\parallel}^{(B1)} \rightarrow O_{\perp, \mu}^{(B1)}. \quad (19)$$

The interpolating currents $j_{\xi q, \perp\nu\rho}^{(0,2)}$ and the necessary SCET weak currents are given by

$$\begin{aligned} j_{\xi q, \perp\nu\rho}^{(0)} &= \bar{\xi} \frac{\not{q}}{2} \gamma_{\perp\rho} \xi \bar{n}_{\nu}, \quad j_{\xi q, \perp\nu\rho}^{(2)} = \left(\bar{\xi}W_c \frac{\not{q}}{2} \gamma_{\perp\rho} Y_s^\dagger q + \bar{q}Y_s \frac{\not{q}}{2} \gamma_{\perp\rho} W_c^\dagger \xi \right) \bar{n}_{\nu}, \\ O_{\perp, \mu}^{(A0)} &= (\bar{\xi}W_c) \gamma_5 \gamma_{\perp\mu} h_v, \quad O_{\perp, \mu}^{(A1, m_c)} = m_c (\bar{\xi}W_c) \frac{\not{q}}{2} \frac{1}{-in \cdot \overleftarrow{D}_c} \gamma_5 \gamma_{\perp\mu} h_v, \\ O_{\perp, \mu}^{(B1)} &= (\bar{\xi}W_c)(0) \gamma_5 \gamma_{\perp\mu} (W_c^\dagger i\cancel{D}_{c\perp} W_c)(rn) h_v(0). \end{aligned} \quad (20)$$

Interestingly, the effective form factor ξ_{\perp, m_c} vanishes at one loop in the four-dimensional space-time. The resulting SCET sum rules for the effective transverse form factors ξ_{\perp} and Ξ_{\perp} at $\mathcal{O}(\alpha_s)$ can be explicitly written as

$$\xi_{\perp} = \frac{\mathcal{F}_{B_q}(\mu)}{f_{D_q^*, \perp}} \frac{m_{B_q}}{n \cdot p} \int_0^{\omega_s} d\omega' \exp \left[\frac{m_{D_q^*}^2 - n \cdot p \omega'}{n \cdot p \omega_M} \right] \left\{ \left[\phi_{B, \text{eff}}^-(\omega') + \Delta\phi_{B, \text{eff}}^-(\omega') \right] + \frac{m_q}{\omega'} \left[\phi_{B, \text{eff}}^{+, m_q}(\omega') + \Delta\phi_{B, \text{eff}}^{+, m_q}(\omega') \right] \right\},$$

Parameter	Value/Interval	Unit	Prior	Source/Comments
Quark-Gluon Coupling and Quark Masses				
$\alpha_s^{(5)}(m_Z)$	[0.1170, 0.1188]	—	—	[130]
$\overline{m}_b(\overline{m}_b)$	[4.192, 4.214]	GeV	gaussian @ 68%	[130]
$m_b^{\text{PS}}(2 \text{ GeV})$	[4.493, 4.545]	GeV	gaussian @ 68%	[133]
$\overline{m}_c(\overline{m}_c)$	[1.265, 1.291]	GeV	gaussian @ 68%	[84]
$\overline{m}_s(2 \text{ GeV})$	[92.5, 93.7]	MeV	gaussian @ 68%	[130]
$\overline{m}_u(2 \text{ GeV})$	[2.12, 2.28]	MeV	gaussian @ 68%	[130]
$\overline{m}_d(2 \text{ GeV})$	[4.64, 4.74]	MeV	gaussian @ 68%	[130]
Hadron Masses				
m_B	5279.66	MeV	—	[130]
m_{B_s}	5366.92	MeV	—	[130]
m_D	1869.66	MeV	—	[130]
m_{D^*}	2010.26	MeV	—	[130]
m_{D_s}	1968.35	MeV	—	[130]
$m_{D_s^*}$	2112.2	MeV	—	[130]
Decay Constants				
$f_{B_d} _{N_f=2+1+1}$	[0.1887, 0.1913]	GeV	gaussian @ 68%	[84]
$f_{B_s} _{N_f=2+1+1}$	[0.2290, 0.2316]	GeV	gaussian @ 68%	[84]
$f_D _{N_f=2+1+1}$	[0.2113, 0.2127]	GeV	gaussian @ 68%	[84]
$f_{D_s} _{N_f=2+1+1}$	[0.2494, 0.2504]	GeV	gaussian @ 68%	[84]
$f_{D^*,\parallel}$	[0.210, 0.245]	GeV	gaussian @ 68%	[85]
$f_{D^*,\perp}(\nu)$	[0.186, 0.218]	GeV	gaussian @ 68%	[85]
$f_{D_s^*,\parallel}$	[0.260, 0.298]	GeV	gaussian @ 68%	[85]
$f_{D_s^*,\perp}(\nu)$	[0.239, 0.272]	GeV	gaussian @ 68%	[85]
Shape Parameters of the Bottom-Meson LCDAs				
$\lambda_{B_d}(\mu_0)$	[200, 500]	MeV	uniform @ 100%	[75, 134]
$\lambda_{B_s}(\mu_0)$	[250, 550]	MeV	uniform @ 100%	[75, 134]
$\{\hat{\sigma}_1(\mu_0), \hat{\sigma}_2(\mu_0)\}$	$\{[-0.7, -6.0], \{0.7, 6.0\}\}$	—	uniform @ 100%	[75, 134]
$\lambda_E^2(\mu_0)/\lambda_H^2(\mu_0)$	[0.40, 0.60]	—	uniform @ 100%	[70]
$2\lambda_E^2(\mu_0) + \lambda_H^2(\mu_0)$	[100, 400]	MeV	uniform @ 100%	[70]
Sum Rule Parameters and Scales				
μ	[1.0, 2.0]	GeV	uniform @ 100%	[46]
μ_h	$[m_b/2, 2 m_b]$	GeV	$\ln(\mu_h)$ uniform @ 100%	[46]
M^2	[3.5, 5.5]	GeV ²	uniform @ 100%	[43, 44, 89]
$s_0^D(s_0^{D^*})$	[6.5, 7.5]	GeV ²	uniform @ 100%	[43, 44, 89]
$s_0^{D_s}(s_0^{D_s^*})$	[7.0, 8.0]	GeV ²	uniform @ 100%	[87, 88]

TABLE II. Numerical values of the input parameters employed in the LCSR determinations of the exclusive $\bar{B}_q \rightarrow D_q^{(*)} \ell \bar{\nu}_\ell$ form factors. The quoted transverse D_q^* decay constants are evaluated at the renormalization scale $\nu = 1.67 \text{ GeV}$ [85]. The full prior distribution is determined by the product of the uncorrelated individual priors, which are either uniform or Gaussian distributed. The uniform priors cover the listed intervals with 100 % probability, while the Gaussian ones adopt the listed intervals such that the central values correspond to the modes and the intervals contain 68 % of accumulated probability [90, 91].

$$\Xi_{\perp} = -\frac{\alpha_s C_F}{2\pi} \frac{\mathcal{F}_{B_q}(\mu)}{f_{D_q^*,\perp}} \frac{m_{B_q}}{m_b} \bar{\tau} \theta(\tau) \theta\left(\bar{\tau} - \frac{\omega_c}{\omega_s}\right) \int_{\omega_c/\bar{\tau}}^{\omega_s} d\omega' \exp\left[\frac{m_{D_q^*}^2 - n \cdot p \omega'}{n \cdot p \omega_M}\right] \int_{\omega' - \omega_c/\bar{\tau}}^{+\infty} \frac{d\omega}{\omega} \phi_B^+(\omega), \quad (21)$$

where we have introduced two additional coefficient functions $\Delta\phi_{B,\text{eff}}^-$ and $\Delta\phi_{B,\text{eff}}^{+,m_q}$ for brevity

$$\begin{aligned} \Delta\phi_{B,\text{eff}}^-(\omega') &= \frac{\alpha_s C_F}{4\pi} \theta(\omega' - \omega_c) \int_0^\infty d\omega \left\{ \theta(\omega' - \omega - \omega_c) \left(1 - \frac{\omega_c^2}{\omega'^2}\right) \ln \frac{\omega' - \omega - \omega_c}{\omega' - \omega_c} \right. \\ &\quad \left. + \theta(\omega + \omega_c - \omega') \left[\ln \frac{\mu^2}{m_c^2} + \left(1 - \frac{\omega_c^2}{\omega'^2}\right) \ln \frac{\omega_c(\omega + \omega_c - \omega')}{(\omega' - \omega_c)^2} + \frac{\omega_c}{\omega'} \right] \right\} \frac{d}{d\omega} \phi_B^-(\omega) + \mathcal{O}(\alpha_s^2), \\ \Delta\phi_{B,\text{eff}}^{+,m_q}(\omega') &= \frac{\alpha_s C_F}{4\pi} \theta(\omega' - \omega_c) \int_0^\infty d\omega \left\{ \theta(\omega' - \omega - \omega_c) \left[\frac{\omega_c(\omega' - \omega_c)}{\omega'} \ln \frac{\omega' - \omega_c}{\omega' - \omega_c - \omega} \frac{d}{d\omega} \frac{\phi_B^+(\omega)}{\omega} + \frac{\omega \omega_c}{\omega' - \omega} \frac{\phi_B^+(\omega)}{\omega^2} \right] \right. \\ &\quad \left. + \theta(\omega + \omega_c - \omega') \left[\frac{\omega_c(\omega' - \omega_c)}{\omega'} \ln \frac{(\omega' - \omega_c)^2}{\omega_c(\omega + \omega_c - \omega')} \frac{d}{d\omega} \frac{\phi_B^+(\omega)}{\omega} + \frac{\omega' - \omega_c}{\omega} \frac{d}{d\omega} \phi_B^+(\omega) \right] \right\} + \mathcal{O}(\alpha_s^2). \quad (22) \end{aligned}$$

Detailed Numerical Results for the Exclusive Bottom-Meson Decay Form Factors

We summarize explicitly the numerical values of all input parameters employed in our LCSR analysis and their prior density functions in Table II, including further their sources. As already discussed in the main text, the statistical procedure previously discussed in [90, 91] is then implemented to determine the mean values and theoretical uncertainties for the form factors of our interest. In order to facilitate the future phenomenological explorations, we collect the yielding numerical results of the semileptonic $\bar{B}_{(s)} \rightarrow D_{(s)}^{(*)}$ decay form factors as well as their correlation matrix at the six representative kinematic points $q^2 \in \{-3.0, -2.0, -1.0, 0.0, 1.0, 2.0\}$ GeV² from our NLL \oplus NLP LCSR computations in the ancillary file `InputLCSR.txt` attached to the arXiv preprint version of this letter. Our numerical explorations indicate that the dominating theory uncertainties of the current LCSR computations for the exclusive $b \rightarrow c\ell\bar{\nu}_\ell$ form factors arise from the variations of non-perturbative shape parameters dictating the two-particle bottom-meson distribution amplitudes in HQET. The most prominent feature of our LCSR predictions consists in the strong correlations of the obtained data points at the different q^2 -values, which can be attributed to the universal hadronic inputs appearing in the analytical sum rules for the complete set of the $\bar{B}_q \rightarrow D_q^{(*)}$ form factors. This essential pattern is in sharp contrast with the more conventional sum rules for the heavy-to-light B -meson form factors, employing the light-meson distribution amplitudes in QCD [135–139]. It is then naturally expected that the obtained correlation matrix for the LCSR data points would be insensitive to the parton-hadron duality violation contributions (see [92–101] for further discussions in different contexts). On the phenomenological aspect, the duality violation contribution in the LCSR framework can be probed by adopting the different alternatives for the duality ansatz with the inclusion of the radial excited or continuum states and with the increased effective threshold [140].

In addition, we provide manifestly the correlation matrices of the obtained BGL expansion coefficients for the $\bar{B}_{(s)} \rightarrow D_{(s)}^{(*)}$ form factors with the three different fitting strategies (as discussed in the main text) in the ancillary file `BGLCoeff.txt` attached to the arXiv preprint version for completeness. Having at our disposal the correlated z -series coefficients, we are then prepared to arrive at the major phenomenological predictions for the considered form factors and the gold-plated LFU quantities as presented in Figure 2 and 3 of the main text.